# Transport of ice into the stratosphere and the humidification of the stratosphere over the 21st century

A.E. Dessler[1], H. Ye[1], T. Wang[2], M.R. Schoeberl[3],
L.D. Oman[4], A.R. Douglass[4],
A.H. Butler[5,6], K.H. Rosenlof[5], S.M. Davis[5,6], R.W. Portmann[5]

[1]Dept. of Atmospheric Sciences, Texas A&M University, College Station, TX
[2]NASA Jet Propulsion Laboratory / Caltech, Pasadena, CA
[3]Science and Technology Corporation, Columbia, MD
[4]NASA Goddard Space Flight Center, Greenbelt, MD
[5]NOAA Earth System Research Lab, Boulder, CO
[6]Cooperative Institute for Research in Environmental Sciences, Univ. of Colorado, Boulder, CO

*Correspondence to: adessler@tamu.edu.

**Abstract**: Climate models predict that tropical lower-stratospheric humidity will increase as the climate warms. We examine this trend in two state-of-the-art chemistry-climate models. Under high greenhouse gas emissions scenarios, the stratospheric entry value of water vapor increases by ~1 part per million by volume (ppmv) over this century in both models. We show with trajectory runs driven by model meteorological fields that the warming tropical tropopause layer (TTL) explains 50-80% of this increase. The remainder is a consequence of trends in evaporation of ice convectively lofted into the TTL and lower stratosphere. Our results further show that, within the models we examined, ice lofting is primarily important on long time scales — on interannual time scales, TTL temperature variations explain most of the variations in lower stratospheric humidity. Assessing the ability of models to realistically represent ice-lofting processes should be a high priority in the modeling community.

## Introduction

Air traveling from the tropical troposphere into the tropical stratosphere transits the tropical tropopause layer (TTL) [Sherwood and Dessler, 2000], and the processes within this region provide primary control over the water vapor content of the stratosphere. In the following, we will refer to the water vapor mixing ratio of this air as $H_2O_{entry}$. Over the past two decades, it has become generally accepted that $H_2O_{entry}$ variability is controlled by TTL temperature variability [e.g., Fueglistaler et al., 2009; Mote et al., 1996; Randel et al., 2004; Fueglistaler et al., 2005; Dessler et al., 2014; Wang et al., 2015]. This view posits that the TTL acts like a "cold trap," where the humidity of lower stratospheric air is determined by the coldest temperatures experienced by the air as it crossed the TTL.

Climate models have long predicted that $H_2O_{entry}$ will increase over the next century [Gettelman et al., 2010; Kim et al., 2013], with important climatic [Forster and Shine, 1999; Solomon et al., 2010; Maycock et al., 2013; Dessler et al., 2013] and chemical [Kirk-Davidoff et al., 1999] impacts. Despite the importance of these model results, few papers have analyzed the mechanism behind the overall increase in $H_2O_{entry}$. Most papers that do view the problem qualitatively, finding that the increase in $H_2O_{entry}$ is roughly consistent with the long-term warming of the TTL [e.g., Fueglistaler and Haynes, 2005; Oman et al., 2008; Gettelman et al., 2009; Garfinkel et al., 2013].

In this paper, we use a trajectory model driven by meteorology taken from climate models to quantitatively evaluate how much of the model trend in $H_2O_{entry}$ is due to changes in TTL temperatures and how much is due to water transport by other processes. We find strong evidence that while much of the future trend is due to a warming TTL, a significant fraction is due to increased transport of water in the form of convectively lofted ice.

## Models

We analyze simulations from two chemistry-climate models (CCMs). These are similar to general circulation models, but with a more realistic stratosphere and higher vertical resolution in the TTL. As such, we expect CCMs to do a better job simulating $H_2O_{entry}$ than general circulation models.

## GEOSCCM

The Goddard Earth Observing System Chemistry Climate Model (GEOSCCM) couples the GEOS-5 general circulation model [Rienecker et al., 2008; Molod et al., 2012] to a comprehensive stratospheric chemistry module. The simulation used in this study has horizontal resolution of 2° latitude and 2.5° longitude with 72 vertical layers up to 0.01 hPa (80 km), with vertical resolution in the TTL of ~1 km. For our estimate of the GEOSCCM's $H_2O_{entry}$, we use the tropical average (30°N-30°S) 85-hPa volume mixing ratios. Averaging over 20°N-20°S yields nearly indistinguishable results.

Prior versions of GEOSCCM have been extensively evaluated as part of the Chemistry-Climate Model Validation 1 (CCMVal-1) [Eyring et al., 2006] and CCMVal-2 [SPARC CCMVal, 2010], as well as in many other analyses [Strahan et al., 2011; Douglass et al., 2012; Oman and Douglass, 2014]. In this paper, we use a simulation from 1998-2099 driven by the RCP6.0 scenario for greenhouse gases [van Vuuren et al., 2011] and the A1 scenario for ozone depleting substances [World Meteorological Organization, 2011]. Sea surface temperatures and sea ice concentrations were prescribed from a CMIP5 simulation using the Community Earth System Model version 1 [Gent et al., 2011].

## WACCM

The Whole Atmosphere Community Climate Model (WACCM) is one of the available atmospheric components of the National Center for Atmospheric Research (NCAR) Community Earth System Model (CESM). WACCM includes processes essential to the simulation of the middle atmosphere such as nonlocal thermodynamic equilibrium radiative transfer, a non-orographic gravity wave drag parameterization, and a full representation of middle atmospheric chemistry that is coupled with radiation and dynamics [Hurrell et al., 2013; Marsh et al., 2013]. The simulation used here is a specified-chemistry version of WACCM (SC-WACCM) where the concentrations of radiatively/chemically active trace gasses are specified from existing WACCM simulations with interactive chemistry [Smith et al., 2014]. SC-WACCM was run at a horizontal resolution of 1.9° x 2.5° over 1955-2100 with the RCP 8.5 greenhouse gas scenario [van Vuuren et al., 2011]. This is a higher emissions scenario than that used in the GEOSCCM run, although

the effect of this on the analysis seems minor. The WACCM simulation includes a fully coupled ocean, land surface, and sea ice model as the other CESM components. For our estimate of the WACCM's $H_2O_{entry}$, we use the same definition as for the GEOSCCM: tropical average (30°N-30°S) 85-hPa volume mixing ratios.

**The trajectory model**

We will compare estimates of $H_2O_{entry}$ from the CCMs to estimates from a domain-filling forward trajectory model [Schoeberl and Dessler, 2011]. In the version of the model analyzed here, an ensemble of 1350 parcels is initialized every day on an equal-area grid running from 60°S to 60°N. The parcels are initialized at 370-K potential temperature (~16 km), which is above the level of zero net radiative heating in the tropics (~355-360 K) but below the tropical tropopause (~375-380 K). Each parcel is run forward until the parcel descends back into the troposphere, defined as pressures higher than 250 hPa (~10 km). All trajectory model runs include production of water vapor via methane oxidation, but that process is unimportant in the tropical lower stratosphere.

The model uses the Bowman trajectory code [Bowman, 1993; Bowman and Carrie, 2002] to advect parcels, driven by 6-hourly instantaneous horizontal winds and 6-hourly average diabatic heating rates obtained from the GEOSCCM and WACCM runs. Each parcel is initialized with a water vapor mixing ratio of 200 parts per million by volume (ppmv). The mixing ratio is conserved along each trajectory, except when the relative humidity (RH) over ice of the parcel exceeds a pre-determined threshold [e.g., Schoeberl and Dessler, 2011], in this paper either 100% or 80%. When parcels' water vapor exceeds this threshold, the water vapor mixing ratio is instantly reduced until the RH equals the threshold value. The 100% threshold is frequently used in these types of analyses, but some CCMs begin dehydration below 100% [e.g., Molod, 2012], so this gives us some idea of the sensitivity of our results to differing thresholds. To estimate $H_2O_{entry}$, we average the $H_2O$ mixing ratio of parcels between 79 and 93 hPa and between 30°N and 30°S. Dehydration events above 93 hPa do occur, but they remove relatively small amounts of water: the water vapor mixing ratio at 79 hPa is within a few percent of the value at 93 hPa.

We will refer to the model described in the previous paragraph as the 100% or 80% standard trajectory model, depending on the dehydration threshold. Despite the simplicity of this model, it has been shown to accurately reproduce many of the details of the water vapor distribution of the stratosphere [Schoeberl and Dessler, 2011]. Table 1 lists 21st-century average $H_2O_{entry}$ in the standard trajectory models and the CCMs. The standard trajectory models do a good job of reproducing the CCMs' value — to the extent they differ, the standard trajectory models tend to underestimate the CCMs. Most observational comparisons focus on water vapor anomalies (departures from the mean seasonal cycle), and the standard trajectory model does an excellent job reproducing observed anomalies [Schoeberl et al., 2012; Schoeberl et al., 2013; Dessler et al., 2014; Wang et al., 2015].

## CCM vs. trajectory model comparison

The GEOSCCM predicts a change in $H_2O_{entry}$ over the 21st century (hereafter $\Delta H_2O_{entry}$) of 0.87 ppmv, while the 100% and 80% standard trajectory model driven by GEOSCCM meteorology predicts $\Delta H_2O_{entry}$ of 0.49 and 0.39 ppmv. The WACCM predicts $\Delta H_2O_{entry}$ of 1.09 ppmv, while the 100% and 80% standard trajectory models driven by WACCM meteorology predicts $\Delta H_2O_{entry}$ of 0.86 and 0.70 ppmv. For all models, $\Delta H_2O_{entry}$ is calculated as $H_2O_{entry}$ averaged over 2090-2100 minus the average over 2000-2010; values are also listed in Table 1.

The disagreement between the CCMs and 100% standard trajectory model is shown graphically in Fig. 1. In the standard trajectory model, $H_2O_{entry}$ is entirely regulated by TTL temperature variations. The fact that the trajectory model mostly follows the GEOSCCM's and WACCM's $H_2O_{entry}$ variations lead us to our first main conclusion: TTL temperature variations are responsible for much of the trend in $H_2O_{entry}$ in the CCMs over the 21st century. However, TTL temperature variations cannot explain all of the trends. In the GEOSCCM and WACCM, about 50% and 20%, respectively, of the 21st-century trend must be due to other processes.

A potential hint to explaining the discrepancy between the CCMs and the standard trajectory model is shown in Figure 2, which shows that convectively lofted ice-water content (IWC) in the GEOSCCM's lower stratosphere increased significantly during the 21st century. Convectively lofted IWC at 100 hPa more than doubles during the 21st century and increases by a factor of

about four at 85 hPa. The WACCM (not shown) only provides total IWC (the sum of convective and *in situ* ice) and that also shows an increase over the 21st century.

The convective injection of ice into the lower stratosphere, above the trajectories' Lagrangian cold-point (LCP), where it can evaporate and moisten the stratosphere [e.g., Dessler et al., 2007; Schoeberl et al., 2014; Ueyama et al., 2015] may be the process missing from the standard trajectory model. LCPs in the 100% standard trajectory runs are found between 110 and 70 hPa, so the observations of convective ice at 100 and 85 hPa are consistent with this hypothesis.

To test this idea, we run a second version of the trajectory model that includes the effects of convectively lofted ice, hereafter referred to as the "trajectory+ice model". In this model, we take the CCMs' 6-hourly three-dimensional ice-water content (IWC) field and interpolate it onto each trajectory time step by linear interpolation in both time and space. At each time step, we assume complete evaporation of this ice into the parcel by adding the CCM's IWC to the parcel's water vapor, although we do not let parcels' RH exceed the RH threshold, either 100% or 80%. Because we assume instant evaporation of the ice, we consider this to be an upper limit of the impact of convective ice evaporation on the water content of the TTL and lower stratosphere.

Figure 1 shows that $\Delta H_2O_{entry}$ from the 80% trajectory+ice model's agrees more closely with the CCMs than either standard trajectory model (also seen in Table 1). The 100% trajectory+ice model (not shown) predicts slightly higher values of $\Delta H_2O_{entry}$ (Table 1). We noted above that the WACCM combines convective and *in situ* ice into one IWC variable, and we use that in the WACCM trajectory+ice model. While this likely causes an overestimate of the evaporated ice in the WACCM-based trajectory models, it may not be significant because *in situ* clouds tend to exist mainly in regions where RH is at or near saturation, so those clouds tend not to be evaporating. Table 1 also shows that the trajectory+ice models predict higher absolute values of $H_2O_{entry}$ than the CCMs, consistent with the idea that the trajectory+ice model is an upper limit on the effect of convective ice lofting.

Figure 3 shows the spatial pattern of the change in $H_2O$ mixing ratio at 100 hPa in the CCMs and two trajectory models over the 21st century. It is clear that the trajectory+ice model more

accurately reproduces the spatial pattern found in both CCMs. The WACCM comparisons are of particular interest. For WACCM, the standard trajectory model actually does a reasonable job simulating the tropical average (e.g., Fig. 1 and Table 1), but Fig. 3 shows that it does a poor job simulating the spatial distribution of water. The trajectory+ice model, on the other hand, does a slightly better job simulating the tropical average, but a much better job reproducing the spatial distribution. The distribution at 85 hPa (not shown) also shows that the trajectory+ice model does a better job simulating the spatial distribution of $H_2O$.

## Are observations consistent with this result?

We have demonstrated that convective ice lofting plays a key role in the long-term evolution of $H_2O_{entry}$ in the CCMs. One obvious question is whether observations are consistent with this. There have been many observational studies showing that convection penetrates into the tropical lower stratosphere [Alcala and Dessler, 2002; Dessler, 2002; Liu and Zipser, 2005; Dessler et al., 2006; Rossow and Pearl, 2007], and there is also evidence that convective injection plays a role regulating the stratospheric water vapor budget [Moyer et al., 1996; Keith, 2000; Johnson et al., 2001; Kuang et al., 2003; Hanisco et al., 2007; Corti et al., 2008; Khaykin et al., 2009; Schoeberl et al., 2014; Ueyama et al., 2015].

At the same time, many other analyses have concluded that observed $H_2O_{entry}$ variations over the last decade or so can be entirely explained by TTL temperature variations [e.g., Fueglistaler et al., 2009; Mote et al., 1996; Randel et al., 2004; Fueglistaler et al., 2005; Dessler et al., 2014; Wang et al., 2015]. This suggests a minor role for convective ice lofting, potentially contradicting results suggesting that convective lofting of ice is important.

We can reconcile this seeming disparity by noting that observational studies necessarily cover short time periods. Over such short periods, the CCMs confirm that TTL temperature variations are indeed the main regulator of $H_2O_{entry}$. This can be seen in Figure 4, which shows monthly $H_2O_{entry}$ anomalies from 2045-2055 from the CCMs agree with those from both the 100% standard trajectory model and the 80% trajectory+ice model. The clear message is that, while convective ice lofting is important for the long-term trend in $H_2O_{entry}$ in the CCMs, it does not play an important role in the CCMs' short-term interannual variations. Thus, previous

conclusions that TTL temperature variability explains $H_2O_{entry}$ variability — based on a decade or so of data — should not be used to dismiss the potential importance of ice lofting in 21st-century trends.

Nevertheless, the CCMs' predictions of ice lofting into the lower stratosphere have not been quantitatively tested against observations. The CCMs' predictions rely on their convective parameterizations, and until verified with observations, one can reasonably question the realism of their representation of the infrequent but intense convective systems that penetrate the stratosphere. In addition, the vertical resolution of the CCMs may not correctly resolve the top of convection, which could also bias the CCMs' simulations. Validation of ice lofting in the CCMs should therefore be a high priority for the scientific community.

## Conclusions

In this paper, we examine the long-term trend in $H_2O_{entry}$, the humidity of air entering the tropical stratosphere, in two state-of-the-art chemistry-climate models (CCMs). The two models, the GEOSCCM and WACCM, both predict $H_2O_{entry}$ will increase over the 21st century by ~1 ppmv.

One hypothesis is that this trend is caused by a warming tropical tropopause layer (TTL). We test this by comparing $H_2O_{entry}$ from the CCM to that predicted by our trajectory models driven by the CCMs' meteorology. The trajectory model sets water in each parcel to the minimum saturation mixing ratio the parcel experienced as it transited the TTL. We find that the warming of the TTL during the 21st century does indeed increase $H_2O_{entry}$, but explains only 50-80% of the CCMs' trends in $H_2O_{entry}$. The remainder of the CCMs' trends in $H_2O_{entry}$ must therefore be due to other processes.

We identify the other process to be an increase in convectively lofted ice. If lofted above the Lagrangian cold point, the ice evaporates and moistens the stratosphere. Supporting this hypothesis is the fact that the CCMs predict increases in convectively lofted ice in the lower stratosphere. We tested the impact of this process by modifying the trajectory model to allow for the evaporation of convective ice. This trajectory+ice model does a much better job simulating both the magnitude of the 21st century trends and the spatial pattern.

We believe that solid evidence exists that trends in convectively lofted ice evaporation drives a significant part of the 21st-century trend in $H_2O_{entry}$ in the CCMs. This is mainly a long-term effect — on short time scales, the CCMs and trajectory models agree that TTL temperature variability drives most of the $H_2O_{entry}$ variability. This makes quantifying the impact of ice lofting in observational records difficult because observational records are generally too short for ice lofting to play a major role. Nevertheless, the importance of ice lofting on the long-term evolution of $H_2O_{entry}$ in CCMs should provide ample motivation to the community to study the fidelity of the CCMs' representation of this process.

**Acknowledgments**: This work was supported by NSF grant AGS-1261948 and NASA grant NNX13AK25G, both to Texas A&M University. Monthly data used in this paper are archived at https://goo.gl/sjcpiJ.

## References

Alcala, C. M., and A. E. Dessler (2002), Observations of deep convection in the tropics using the TRMM precipitation radar, J. Geophys. Res., 107, 4792, doi: 10.129/2002JD002457.

Bowman, K. P. (1993), Large-scale isentropic mixing properties of the Antarctic polar vortex from analyzed winds, J. Geophys. Res., 98, 23013-23027.

Bowman, K. P., and G. D. Carrie (2002), The mean-meridional transport circulation of the troposphere in an idealized GCM, J. Atmos. Sci., 59, 1502-1514.

Corti, T., et al. (2008), Unprecedented evidence for deep convection hydrating the tropical stratosphere, Geophys. Res. Lett., 35, L10810, doi: 10.1029/2008gl033641.

Dessler, A. E. (2002), The effect of deep, tropical convection on the tropical tropopause layer, J. Geophys. Res., 107, 4033, doi: 10.1029/2001JD000511.

Dessler, A. E., S. P. Palm, and J. D. Spinhirne (2006), Tropical cloud-top height distributions revealed by the Ice, Cloud, and Land Elevation Satellite (ICESat)/Geoscience Laser Altimeter System (GLAS), J. Geophys. Res., 111, D12215, doi: 10.1029/2005JD006705.

Dessler, A. E., T. F. Hanisco, and S. Fueglistaler (2007), Effects of convective ice lofting on $H_2O$ and HDO in the tropical tropopause layer, J. Geophys. Res., 112, D18309, doi: 10.1029/2007JD008609.

Dessler, A. E., M. R. Schoeberl, T. Wang, S. M. Davis, and K. H. Rosenlof (2013), Stratospheric water vapor feedback, Proc. Natl. Acad. Sci., 110, doi: 10.1073/pnas.1310344110, 18087-18091.

Dessler, A. E., M. R. Schoeberl, T. Wang, S. M. Davis, K. H. Rosenlof, and J.-P. Vernier (2014), Variations in stratospheric water vapor over the past three decades, J. Geophys. Res., 119, doi: 10.1002/2014JD021712., 12,588–512,598.

Douglass, A. R., R. S. Stolarski, S. E. Strahan, and L. D. Oman (2012), Understanding differences in upper stratospheric ozone response to changes in chlorine and temperature as computed using CCMVal-2 models, J. Geophys. Res., 117, D16306, doi: 10.1029/2012jd017483.

Eyring, V., et al. (2006), Assessment of temperature, trace species, and ozone in chemistry-climate model simulations of the recent past, J. Geophys. Res., 111, D22308, doi: 10.1029/2006jd007327.

Forster, P. M. D., and K. P. Shine (1999), Stratospheric water vapour changes as a possible contributor to observed stratospheric cooling, Geophys. Res. Lett., 26, 3309-3312.

287 Fueglistaler, S., and P. H. Haynes (2005), Control of interannual and longer-term variability of stratospheric water
288 vapor, J. Geophys. Res., 110, D24108, doi: 10.1029/2005JD006019.
289 Fueglistaler, S., M. Bonazzola, P. H. Haynes, and T. Peter (2005), Stratospheric water vapor predicted from the
290 Lagrangian temperature history of air entering the stratosphere in the tropics, J. Geophys. Res., 110, D08107,
291 doi: 10.1029/2004JD005516.
292 Fueglistaler, S., A. E. Dessler, T. J. Dunkerton, I. Folkins, Q. Fu, and P. W. Mote (2009), The tropical tropopause
293 layer, Rev. Geophys., 47, RG1004, doi: 10.1029/2008RG000267.
294 Garfinkel, C. I., D. W. Waugh, L. D. Oman, L. Wang, and M. M. Hurwitz (2013), Temperature trends in the tropical
295 upper troposphere and lower stratosphere: Connections with sea surface temperatures and implications for
296 water vapor and ozone, Journal of Geophysical Research: Atmospheres, 118, doi: 10.1002/jgrd.50772, 9658-
297 9672.
298 Gent, P. R., et al. (2011), The Community Climate System Model Version 4, J. Climate, 24, doi:
299 10.1175/2011jcli4083.1, 4973-4991.
300 Gettelman, A., et al. (2009), The Tropical Tropopause Layer 1960-2100, Atmos. Chem. Phys., 9, 1621-1637.
301 Gettelman, A., et al. (2010), Multimodel assessment of the upper troposphere and lower stratosphere: Tropics and
302 global trends, J. Geophys. Res., 115, D00M08, doi: 10.1029/2009jd013638.
303 Hanisco, T. F., et al. (2007), Observations of deep convective influence on stratospheric water vapor and its isotopic
304 composition, Geophys. Res. Lett., 34, L04814, doi: 10.1029/2006GL027899.
305 Hurrell, J. W., et al. (2013), The Community Earth System Model: A framework for collaborative research, Bull.
306 Am. Met. Soc., 94, doi: 10.1175/BAMS-D-12-00121.1, 1339-1360.
307 Johnson, D. G., K. W. Jucks, W. A. Traub, and K. V. Chance (2001), Isotopic composition of stratospheric water
308 vapor: Implications for transport, J. Geophys. Res., 106, 12,219-212,226.
309 Keith, D. W. (2000), Stratosphere-Troposphere exchange: Inferences from the isotopic composition of water vapor,
310 J. Geophys. Res., 105, 15,167-115,173.
311 Khaykin, S., J. P. Pommereau, L. Korshunov, V. Yushkov, J. Nielsen, N. Larsen, T. Christensen, A. Garnier, A.
312 Lukyanov, and E. Williams (2009), Hydration of the lower stratosphere by ice crystal geysers over land
313 convective systems, Atmos. Chem. Phys., 9, doi: 10.5194/acp-9-2275-2009, 2275-2287.
314 Kim, J., K. M. Grise, and S. W. Son (2013), Thermal characteristics of the cold-point tropopause region in CMIP5
315 models, J. Geophys. Res., 118, doi: 10.1002/jgrd.50649, 8827-8841.
316 Kirk-Davidoff, D. B., E. J. Hintsa, J. G. Anderson, and D. W. Keith (1999), The effect of climate change on ozone
317 depletion through changes in stratospheric water vapour, Nature, 402, 399-401.
318 Kuang, Z., G. C. Toon, P. O. Wennberg, and Y. L. Yung (2003), Measured HDO/H2O ratios across the tropical
319 tropopause, in Geophys. Res. Lett., edited, p. 10.1029/2003GL017023.
320 Liu, C., and E. J. Zipser (2005), Global distribution of convection penetrating the tropical tropopause, in J. Geophys.
321 Res., edited, p. 10.1029/2005JD006063.
322 Marsh, D. R., M. J. Mills, D. E. Kinnison, J.-F. Lamarque, N. Calvo, and L. M. Polvani (2013), Climate Change
323 from 1850 to 2005 simulated in CESM1 (WACCM), J. Climate, 26, doi: 10.1175/JCLI-D-12-00558.1, 7372-
324 7391.
325 Maycock, A. C., M. M. Joshi, K. P. Shine, and A. A. Scaife (2013), The circulation response to idealized changes in
326 stratospheric water vapor, J. Climate, 26, doi: 10.1175/jcli-d-12-00155.1, 545-561.
327 Molod, A. (2012), Constraints on the profiles of total water PDF in AGCMs from AIRS and a high-resolution
328 model, J. Climate, 25, doi: 10.1175/JCLI-D-11-00412.1, 8341-8352.
329 Molod, A., L. Takacs, M. Suarez, J. Bacmeister, I.-S. Song, and A. Eichman (2012), The GEOS-5 atmospheric
330 general circulation model: Mean climate and development from MERRA to Fortuna, NASA/TM–2012-
331 104606.
332 Mote, P. W., K. H. Rosenlof, M. E. McIntyre, E. S. Carr, J. C. Gille, J. R. Holton, J. S. Kinnersley, H. C. Pumphrey,
333 J. M. Russell, III, and J. W. Waters (1996), An atmospheric tape recorder: The imprint of tropical tropopause
334 temperatures on stratospheric water vapor, J. Geophys. Res., 101, 3989-4006.
335 Moyer, E. J., F. W. Irion, Y. L. Yung, and M. R. Gunson (1996), ATMOS stratospheric deuterated water and
336 implications for troposphere-stratosphere transport, Geophys. Res. Lett., 23, 2385-2388.
337 Oman, L., D. W. Waugh, S. Pawson, R. S. Stolarski, and J. E. Nielsen (2008), Understanding the changes of
338 stratospheric water vapor in coupled Chemistry-Climate Model simulations, J. Atmos. Sci., 65, doi:
339 10.1175/2008jas2696.1, 3278-3291.
340 Oman, L. D., and A. R. Douglass (2014), Improvements in total column ozone in GEOSCCM and comparisons with
341 a new ozone-depleting substances scenario, J. Geophys. Res., 119, doi: 10.1002/2014jd021590, 5613-5624.

Randel, W. J., F. Wu, S. J. Oltmans, K. Rosenlof, and G. E. Nedoluha (2004), Interannual changes of stratospheric water vapor and correlations with tropical tropopause temperatures, J. Atmos. Sci., 61, 2133-2148.

Rienecker, M. M., et al. (2008), The GEOS-5 data assimilation system — Documentation of versions 5.0.1, 5.1.0, and 5.2.0, NASA/TM–2008–104606.

Rossow, W. B., and C. Pearl (2007), 22-Year survey of tropical convection penetrating into the lower stratosphere, in Geophys. Res. Lett., edited, p. 10.1029/2006GL028635.

Schoeberl, M. R., and A. E. Dessler (2011), Dehydration of the stratosphere, Atmos. Chem. Phys., 11, doi: 10.5194/acp-11-8433-2011, 8433-8446.

Schoeberl, M. R., A. E. Dessler, and T. Wang (2012), Simulation of stratospheric water vapor and trends using three reanalyses, Atmos. Chem. Phys., 12, doi: 10.5194/acp-12-6475-2012, 6475-6487.

Schoeberl, M. R., A. E. Dessler, and T. Wang (2013), Modeling upper tropospheric and lower stratospheric water vapor anomalies, Atmos. Chem. Phys., 13, doi: 10.5194/acp-13-7783-2013, 7783-7793.

Schoeberl, M. R., A. E. Dessler, T. Wang, M. A. Avery, and E. J. Jensen (2014), Cloud formation, convection, and stratospheric dehydration, Earth and Space Science, 1, doi: 10.1002/2014EA000014, 1-17.

Sherwood, S. C., and A. E. Dessler (2000), On the control of stratospheric humidity, Geophys. Res. Lett., 27, 2513-2516.

Smith, K. L., R. R. Neely, D. R. Marsh, and L. M. Polvani (2014), The Specified Chemistry Whole Atmosphere Community Climate Model (SC-WACCM), J. Adv. Model. Earth Syst., 6, doi: 10.1002/2014MS000346, 883-901.

Solomon, S., K. H. Rosenlof, R. W. Portmann, J. S. Daniel, S. M. Davis, T. J. Sanford, and G. K. Plattner (2010), Contributions of stratospheric water vapor to decadal changes in the rate of global warming, Science, 327, doi: 10.1126/science.1182488, 1219-1223.

SPARC CCMVal (2010), SPARC Report on the evaluation of chemistry-climate models, V. Eyring, T.G. Shepherd, D.W. Waugh (Eds.), SPARC Report No. 5, WCRP 132, WMO/TD-No. 1526.

Strahan, S. E., et al. (2011), Using transport diagnostics to understand chemistry climate model ozone simulations, J. Geophys. Res., 116, D17302, doi: 10.1029/2010jd015360.

Ueyama, R., E. J. Jensen, L. Pfister, and J.-E. Kim (2015), Dynamical, convective, and microphysical control on wintertime distributions of water vapor and clouds in the tropical tropopause layer, Journal of Geophysical Research: Atmospheres, 120, doi: 10.1002/2015JD023318, 10,483-410,500.

van Vuuren, D. P., et al. (2011), The representative concentration pathways: an overview, Climatic Change, 109, doi: 10.1007/s10584-011-0148-z, 5-31.

Wang, T., A. E. Dessler, M. R. Schoeberl, W. J. Randel, and J. E. Kim (2015), The impact of temperature vertical structure on trajectory modeling of stratospheric water vapor, Atmos. Chem. Phys., 15, doi: 10.5194/acp-15-3517-2015, 3517-3526.

World Meteorological Organization (2011), Scientific Assessment of Ozone Depletion: 2010, 52, Geneva, Switzerland.

Figure captions

Figure 1. Time series of $\Delta H_2O_{entry}$ from (a) the GEOSCCM and two trajectory model runs driven by GEOSCCM meteorology and (b) from the WACCM and two trajectory model runs driven by WACCM meteorology. $\Delta H_2O_{entry}$ is calculated by subtracting the average of the first 10 years from each time series.

Figure 2. Annual and tropical average convectively lofted ice mixing ratio in parts per billion by volume (ppbv) from the GEOSCCM at 100 hPa (blue line, right-hand axis) and 85 hPa (red line, left-hand axis).

Figure 3. The spatial distribution of the change in $H_2O$ over the 21$^{st}$ century at 100 hPa, calculated as the difference between the average of the last and first decades. Left column: GEOSCCM (top), GEOSCCM 80% trajectory+ice model (middle), GEOSCCM 100% standard trajectory model (bottom). Right column: the same quantities, but from WACCM. Each column's color bar is located at the bottom of the column.

Figure 4. Comparison between the CCMs, 100% standard trajectory model, and 80% trajectory+ice model over one decade (2045-2055). Quantities plotted are anomalies, which are the departures from that decade's mean annual cycle.

401 Table 1. Water vapor comparison between CCMs and trajectory model runs. The first column is
402 $H_2O_{entry}$ averaged over the 21st century. The second column is ($\Delta H_2O_{entry}$) is the change in
403 $H_2O_{entry}$ over the 21st century. The trajectory model listed under GEOSCCM use GEOSCCM
404 meteorology while those listed under WACCM use WACCM meteorology.

| Model | 21st-century avg. $H_2O_{entry}$ (ppmv) | $\Delta H_2O_{entry}$ (ppmv) |
|---|---|---|
| GEOSCCM | 4.1 | 0.87 |
| 100% standard trajectory | 4.2 | 0.49 |
| 80% standard trajectory | 3.3 | 0.39 |
| 100% trajectory+ice | 5.8 | 1.14 |
| 80% trajectory+ice | 4.7 | 0.92 |
| WACCM | 4.7 | 1.09 |
| 100% standard trajectory | 4.0 | 0.86 |
| 80% standard trajectory | 3.2 | 0.70 |
| 100% trajectory+ice | 6.5 | 1.20 |
| 80% trajectory+ice | 5.2 | 0.98 |

405
406

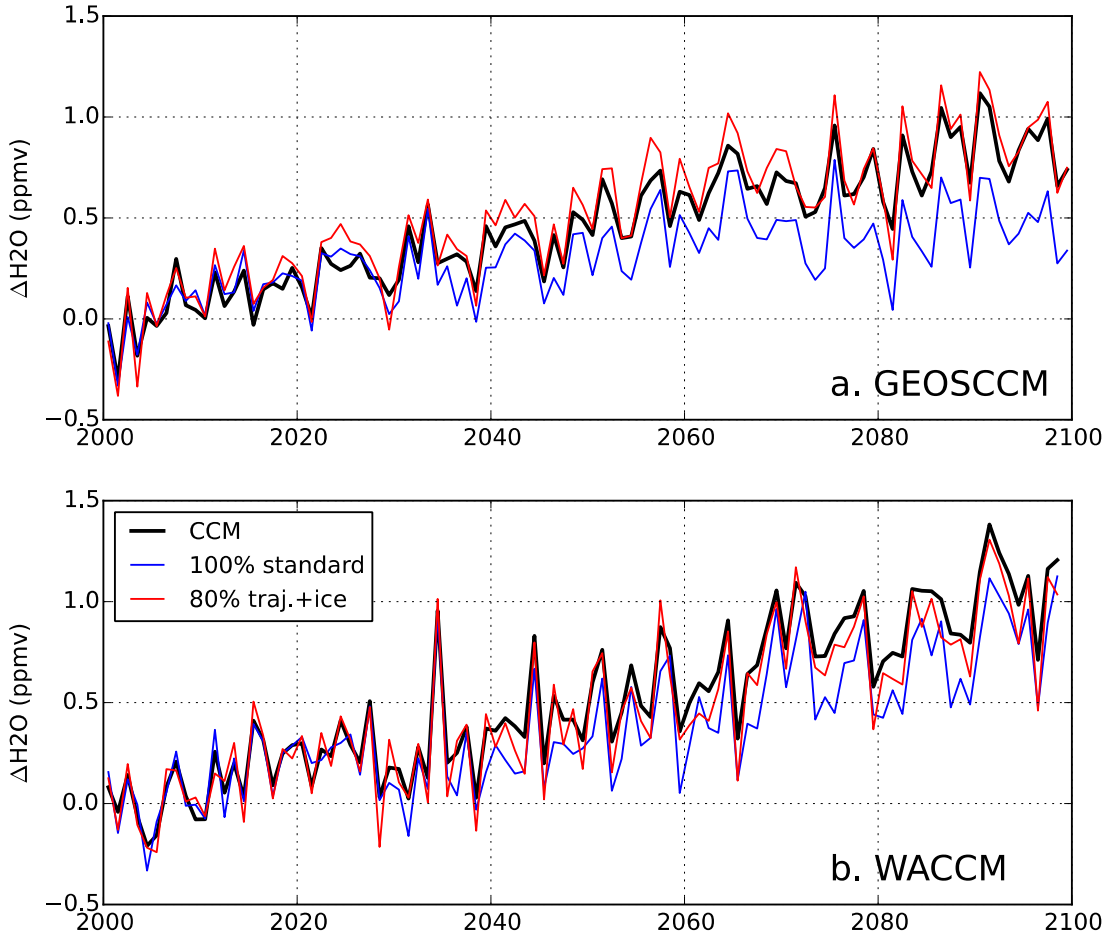


Figure 1. Time series of $\Delta H_2O_{entry}$ from (a) the GEOSCCM and two trajectory model runs driven by GEOSCCM meteorology and (b) from the WACCM and two trajectory model runs driven by WACCM meteorology. $\Delta H_2O_{entry}$ is calculated by subtracting the average of the first 10 years from each time series.

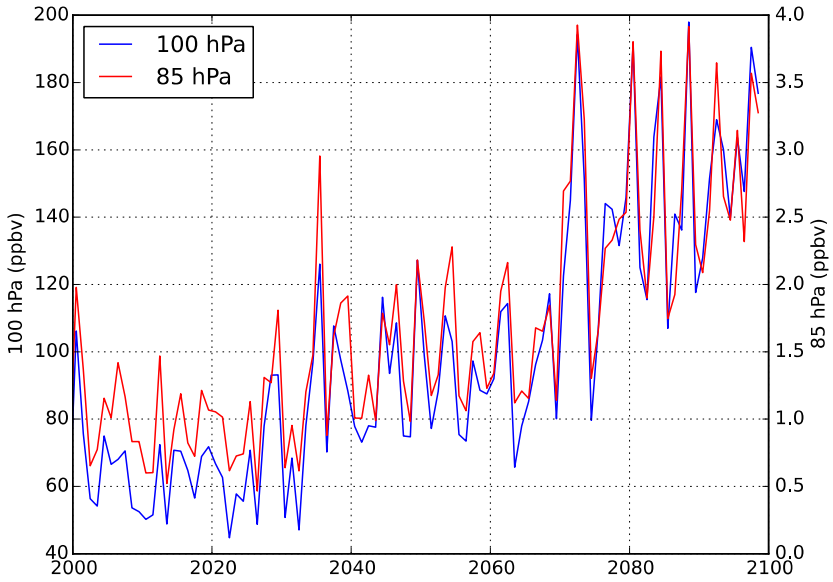


412

413 Figure 2. Annual and tropical average convectively lofted ice mixing ratio in parts per
414 billion by volume (ppbv) from the GEOSCCM at 100 hPa (blue line, right-hand axis)
415 and 85 hPa (red line, left-hand axis).

416

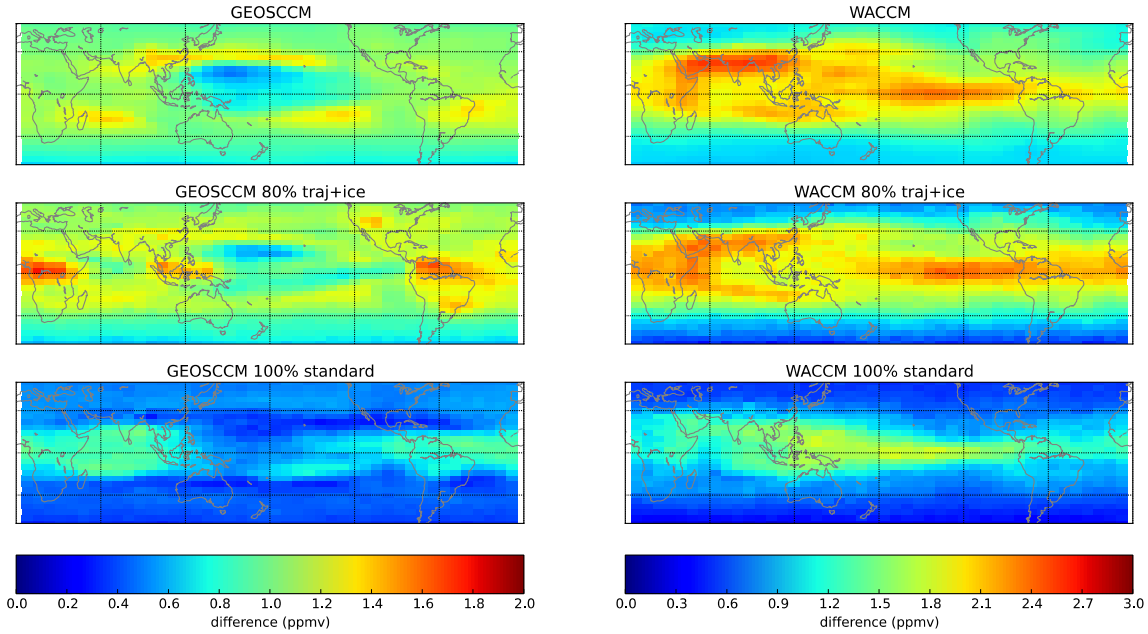


418

419 Figure 3. The spatial distribution of the change in $H_2O$ over the 21$^{st}$ century at 100 hPa,
420 calculated as the difference between the average of the last and first decades. Left column:
421 GEOSCCM (top), GEOSCCM 80% trajectory+ice model (middle), GEOSCCM 100% standard
422 trajectory model (bottom). Right column: the same quantities, but from WACCM. Each
423 column's color bar is located at the bottom of the column.

424

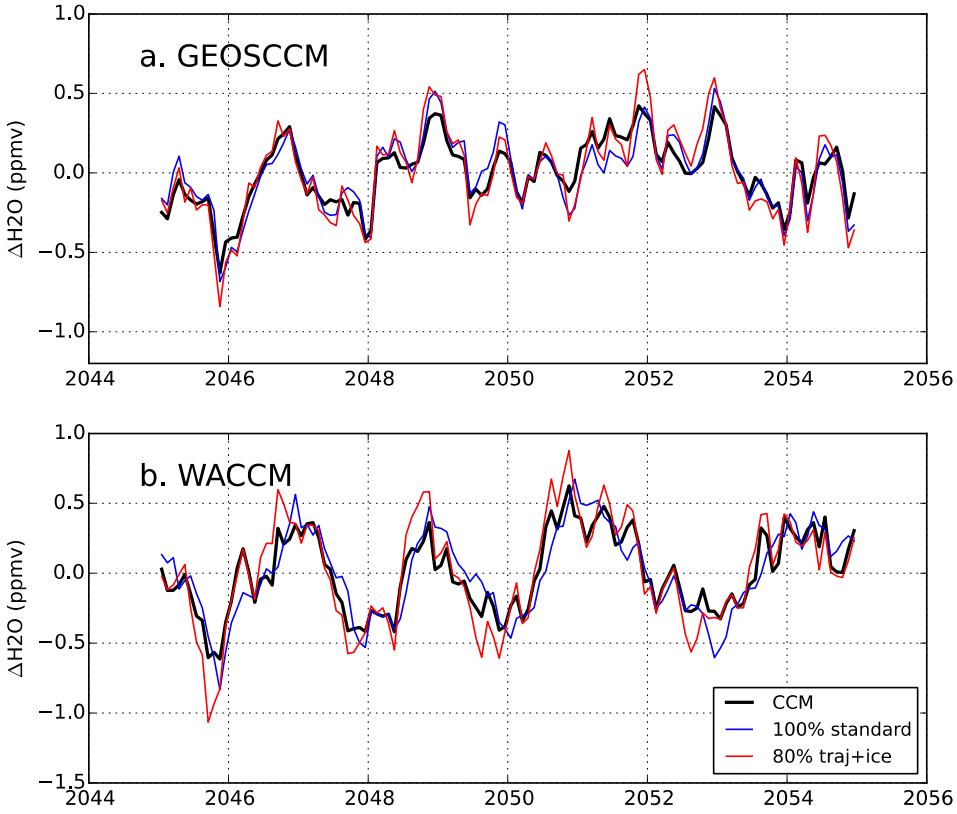


425

426 Figure 4. Comparison between the CCMs, 100% standard trajectory model, and 80%
427 trajectory+ice model over one decade (2045-2055). Quantities plotted are anomalies, which are
428 the departures from that decade's mean annual cycle.

429